

# An Electrically Small Dual-Band Antenna Covered with SRs and SRR

Ke Xiao<sup>1</sup>, Jun Dong<sup>1, 2, \*</sup>, Liang Ding<sup>1</sup>, and Shunlian Chai<sup>1</sup>

**Abstract**—A dual-band antenna operating in dual bands is presented. The antenna is composed of two substrate layers covered with three printed patch layers. The top layer is an electrically small ring; the middle consists of four spiral resonators (SRs); and the bottom is a split-ring resonator (SRR). Inductive couplings between layers change the radiation  $Q$  factor of the original ring antenna and promote resonating modes in UHF and S bands. Besides, the input matching property is also improved. The measured return loss agrees well with the calculated results, and the radiation patterns are also presented. From experiments it is found that the proposed antenna is electrically small at operation dual-bands.

## 1. INTRODUCTION

With a rapid development of modern wireless communication technology, wireless radio frequency identification (RFID) systems, multi-band and compact antennas are increasingly required as an important component in portable and small devices. Most of the applications focus on the requirement of antennas for dual ISM bands, such as lower WLAN 2.4 GHz and upper WLAN 5.2/5.8 GHz. In particular, some wireless applications such as satellite communication have promoted the antenna designed with a small ground plane for dual frequencies in UHF and S bands, respectively. However, it is difficult to achieve combining radiations at the two frequencies in one antenna for handheld use.

For ordinary antennas such as patch, dipole, and monopole antenna, the maximum dimension ( $D_{\max}$ ) is approximately  $\lambda/2$  or  $\lambda/4$ , where  $\lambda$  is the operating wavelength, so traditional designs usually fail to have compact size, which become unportable. Electrically small antennas (ESAs) have attracted much attention [1], due to their reduced size and capability to be integrated on chip. For ESAs, the maximum dimension is much smaller than  $\lambda$ , where  $\lambda$  is the operation wavelength. Specifically, a lossless and resonant ESA with characteristic radius  $a$  is guaranteed to have a quality factor  $Q$  greater than the Chu limit [2], which limits the operation bandwidth less than  $f_0/Q_{\text{Chu}}$  for carrier frequency  $f_0$ . Meanwhile, the ESA's radiation resistance is usually much smaller than the Ohmic loss on the radiation elements, leading to low radiation efficiency.

To improve the performance of ESAs within the Chu limit constraint, efforts are made to find new approaches as follows: 1) Adding parasitic elements, such as split-ring resonators (SRRs) [2–4] and Egyptian axe dipole elements [5]. 2) Metamaterials with negative permeability and permittivity can act as a phase compensator, which can be applied to design sub-wavelength antennas [6–8, 10]. 3) Huygens sources with pairs of magnetic and electric radiators can be utilized to achieve the desired directive outcome [9]. 4) The ESA's capacitance is designed to be increased, and its inductance is suppressed, so as to increase the available relative bandwidth [11]. In [2], coupled SRRs are used to construct ESAs, whose radiation efficiency reaches 41%, with the relative footprint of  $0.05\lambda_0 \times 0.05\lambda_0$ . In [3], an ESA operating at 934 MHz and 1.55 GHz is designed with a small ring and two concentric SRRs on an FR-4

---

Received 7 August 2020, Accepted 15 October 2020, Scheduled 27 October 2020

\* Corresponding author: Jun Dong (jdongcn@outlook.com).

<sup>1</sup> College of Electronic Science, National University of Defense Technology, Changsha 410073, China. <sup>2</sup> College of Information Science and Engineering, Hunan Normal University, Changsha 410081, China.

substrate, and the measured radiation efficiency of the antenna is 36.7% at the lower band and 43.6% at high-band resonant frequency. In [6], an ESA, with compact size of  $0.31\lambda_0 \times 0.08\lambda_0 \times 0.01\lambda_0$  at 1.89 GHz and radiation efficiency equal to 44.6%, can be used to operate at GSM 1800 and Wi-MAX. In [10], two ESAs are designed integrated with a CRLH structure, one operating at 1760, 2550, and 3850 MHz with gains 2.1,  $-3.9$ , and 2.5 dBi and the other operating at 1060, 1800, and 2500 MHz.

In this paper, subwavelength SRs and SRR are loaded to an electrically small loop antenna. In Section 2, the configuration of the proposed antenna is given. Then, the antenna is analyzed and simulated in Section 3, where the design procedure and working principle are described. The physical mechanism behind the antenna is exploited by surface current distribution. Section 4 presents the experimental antenna and radiation performances, where an electrically-small dual-band antenna in UHF and S bands are achieved.

## 2. ANTENNA STRUCTURE

Figure 1 shows the configuration of the proposed antenna, which consists of an electrically small ring in top layer, four SRs in middle layer, and one SRR in bottom layer. The small loop acts as the excitation of radiation, with its center vertically overlapped with that of other layers. The electrically small SR is equivalent to a lumped inductance, and the SRR is equivalent to a lumped LC resonant circuit. To express the effects of SR layer and SRR layer to the ring antenna, some simulation results are presented in the following section. The three layers are supported by two layers of FR-4 substrate, with thickness  $h$  equal to 1.5 mm, and the relative dielectric constant  $\epsilon_r$  is 4.4 with a loss tangent of 0.029. The total size of the antenna is  $35 \times 35 \times 3.07 \text{ mm}^3$  ( $x \times y \times z$ ).

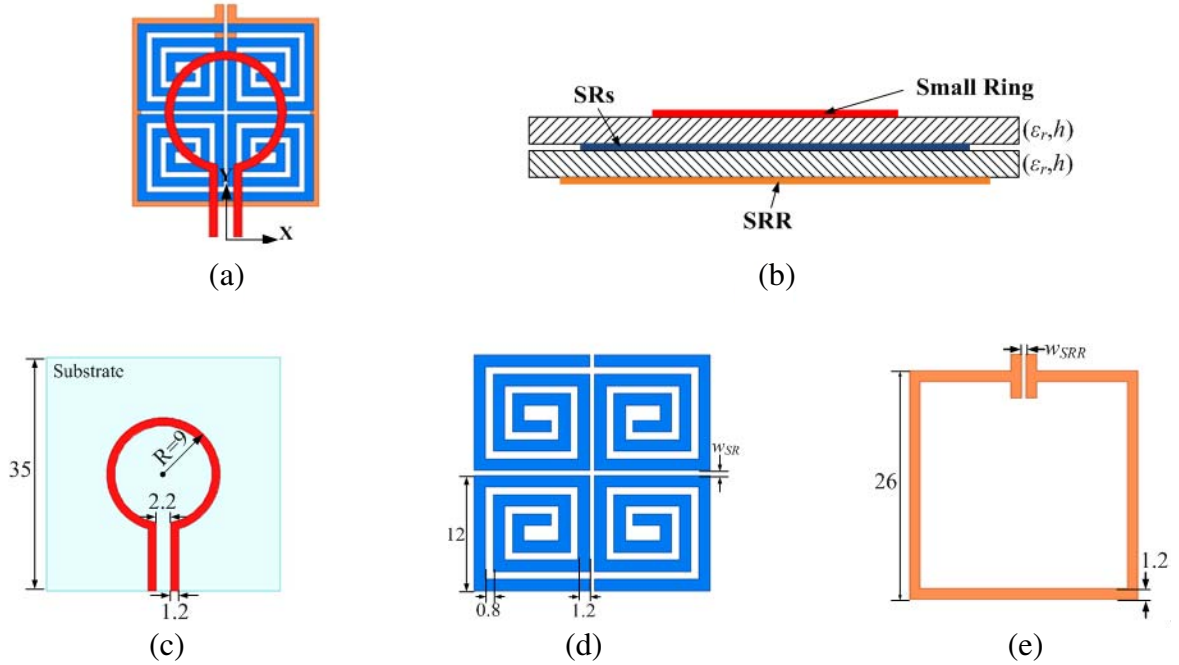


**Figure 1.** Configuration of proposed antenna. (a) Top view with substrate being transparent, (b) side view, (c) top ring, (d) SR layer in middle, (e) SRR layer at bottom. Unit: mm.

## 3. DESIGN AND SIMULATION

From Chu's limit, the  $Q$  factor of an ESA has approximate fundamental limitation as follows:

$$Q = \frac{1}{ka} + \frac{1}{(ka)^3} \quad (1)$$

where  $k = 2\pi/\lambda$  and  $a$  is the radius of the sphere enclosing the antenna. Also, there is a bound termed as ‘Harrington bound’ on the maximum realizable gain due to the electrical size of an ESA [11], which is shown as:

$$G_{\text{dBi}} = 10 \log_{10} \left( (ka)^2 + 2ka \right) \tag{2}$$

For an ESA ( $ka < 1$ ), the maximum feasible gain can be obtained by Eq. (2), and the maximum theoretical bandwidth can be estimated by Eq. (1).

Then, Ansys HFSS was used for simulations of antennas. Firstly, the return loss of the ring antenna depicted in Figure 1(c) was simulated, and the results are shown in Figure 2(a). The resonant frequencies appear at 3.9 GHz and 5.9 GHz, respectively. Then, the SRR layer is added to the ring antenna as shown in Figure 3(a), and the results show that the antenna resonates at the frequency of 835 MHz, with relative bandwidth equal to about 1%. Gap width  $w_{\text{SRR}}$  affects the resonant frequency, and it is set to 0.5 mm here. Similarly, the SRs layer is added to the ring antenna separately, and the

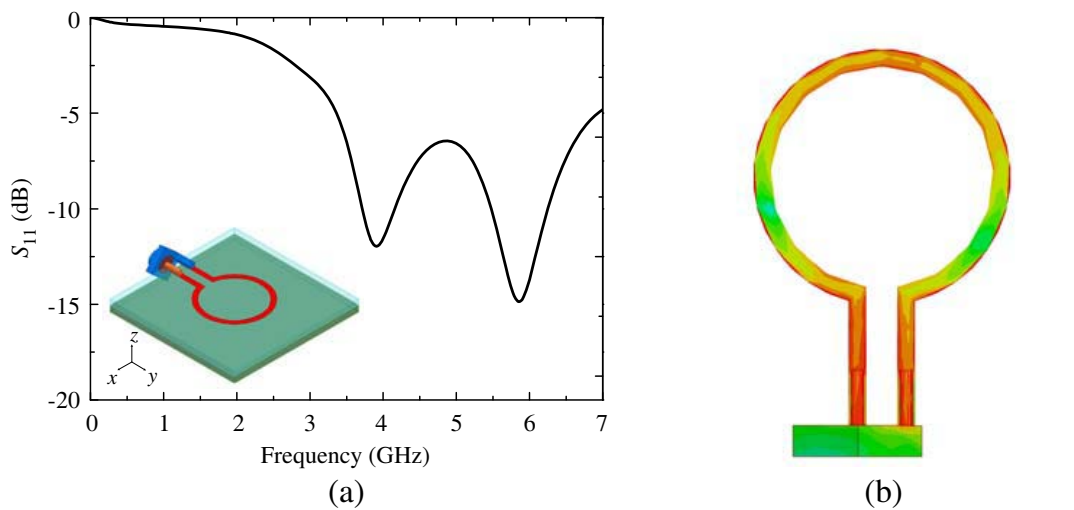


**Figure 2.** Simulation results of ring antenna: (a) reflection coefficients; (b) current distribution of the antenna at 3.9 GHz.

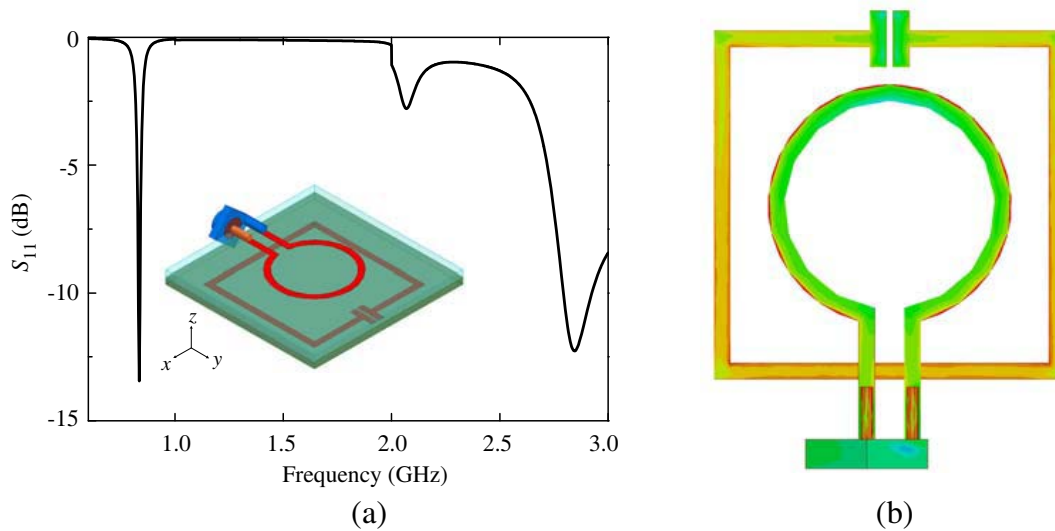


**Figure 3.** Simulation of ring antenna covered with SRR: (a) reflection coefficients in frequency band from 0.5 GHz to 3 GHz; (b) current distribution of the antenna at 0.835 GHz.

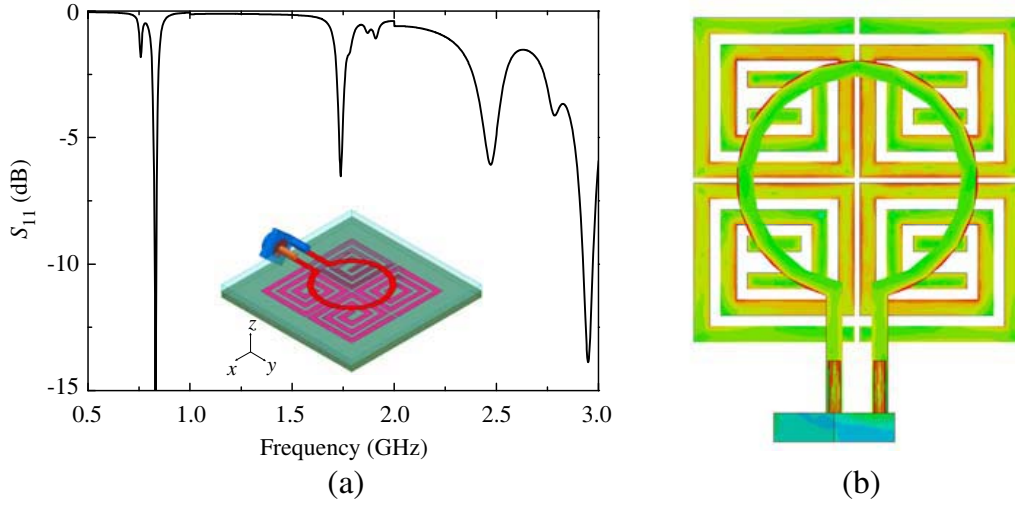


**Figure 4.** Simulation of ring antenna loaded with SRR: (a) reflection coefficients in frequency band from 0.5 GHz to 3 GHz; (b) current distribution of the antenna at 0.832 GHz.

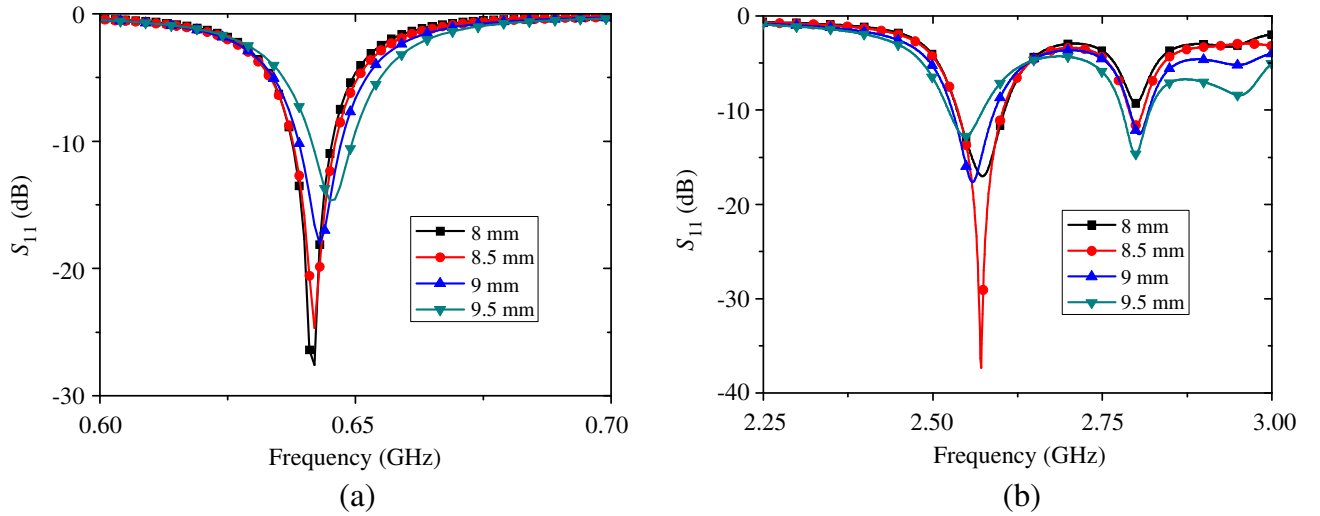


**Figure 5.** Simulated reflection coefficients under different  $R$ : (a) in frequency band from 0.6 GHz to 0.7 GHz; (b) in frequency band from 2.25 GHz to 3.0 GHz.

simulation result is shown in Figure 4(a), in which two resonant frequencies can be observed, 832 MHz and 1.74 GHz, respectively.

From the current distribution shown in Figure 2(b), the resonant mode of the ring antenna can be observed at 3.9 GHz. In Figure 3(b), the SRR structure resonates at the frequency of 0.835 GHz, and the ring acts as a magnetic excited to the whole antenna. The SRs layer in Figure 4(a) can be equal to a lumped LC resonant circuit at the frequency of 0.832 GHz. So the cover of SRs layer or SRR layer can bring a strong inductive coupling to the ring antenna, and resonant frequencies in UHF band and S band can be obtained by changing the parameters of SR and SRR.

Then, the SR layer and SRR are integrated to the ring antenna as shown in Figure 1(a). To further consider the effects of loaded structures, radius ( $R$ ) of the ring as shown in Figure 1(c), gaps ( $w_{SR}$ ) of SRs in middle layer shown in Figure 1(d), and gap ( $w_{SRR}$ ) in SRR layer depicted in Figure 1(e) are changed respectively. The port's reflection coefficients are obtained through HFSS simulations, as shown in Figure 5, Figure 6, and Figure 7, respectively. From Figure 5, we see that by gradually changing

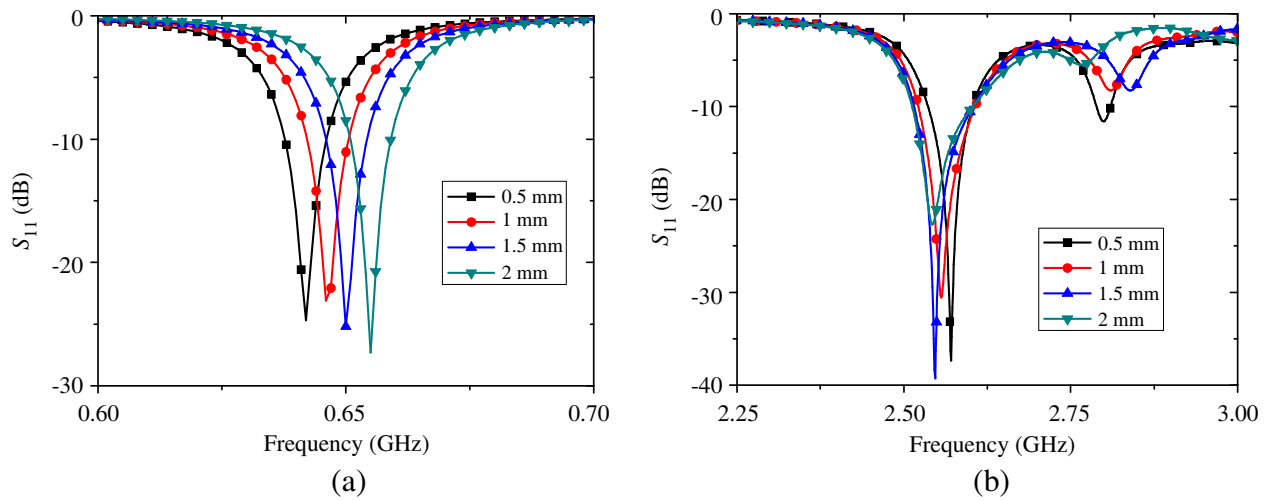


**Figure 6.** Simulated reflection coefficients under different  $w_{SR}$ : (a) in frequency band from 0.6 GHz to 0.7 GHz; (b) in frequency band from 2.25 GHz to 3.0 GHz.

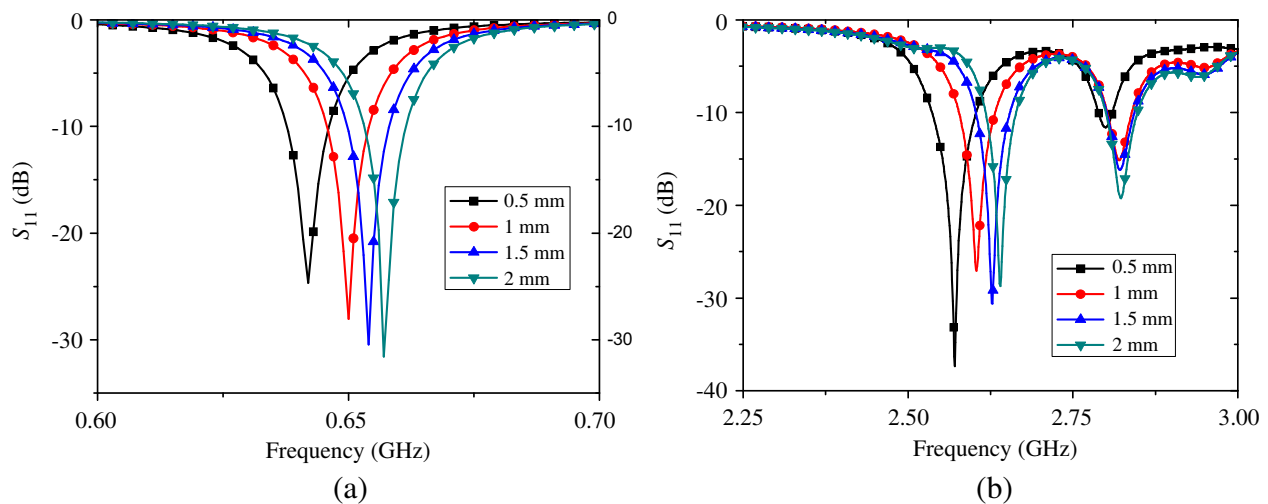


**Figure 7.** Simulated reflection coefficients under different  $w_{SRR}$ : (a) in frequency band from 0.6 GHz to 0.7 GHz; (b) in frequency band from 2.25 GHz to 3.0 GHz.

the radius of ring, the performance of impedance matching changes. From Figure 6, by tuning the gaps of SRs in middle layer, resonant frequency at lower band changes obviously, and as  $w_{SR}$  increase, the resonating frequency goes up. From Figure 7, the frequency goes down as gap spacing  $w_{SRR}$  decreases, because as gap spacing decreases, the equivalent capacitance of SRR increases, so resonating frequency decreases.

In the next section, the simulated results of the model with dimensions shown in Figure 1 will be compared to the measured ones.

#### 4. MEASUREMENT RESULTS AND DISCUSSION

To validate the performance of the proposed dual-band antenna, a designed prototype was fabricated and measured as shown in Figure 8. Both simulated and measured reflection coefficients are presented in Figure 9, and good agreement between them can be observed. The first antenna band exists with the

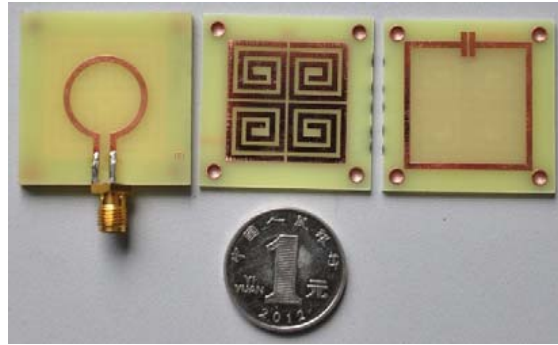


**Figure 8.** Fabricated antenna prototype.

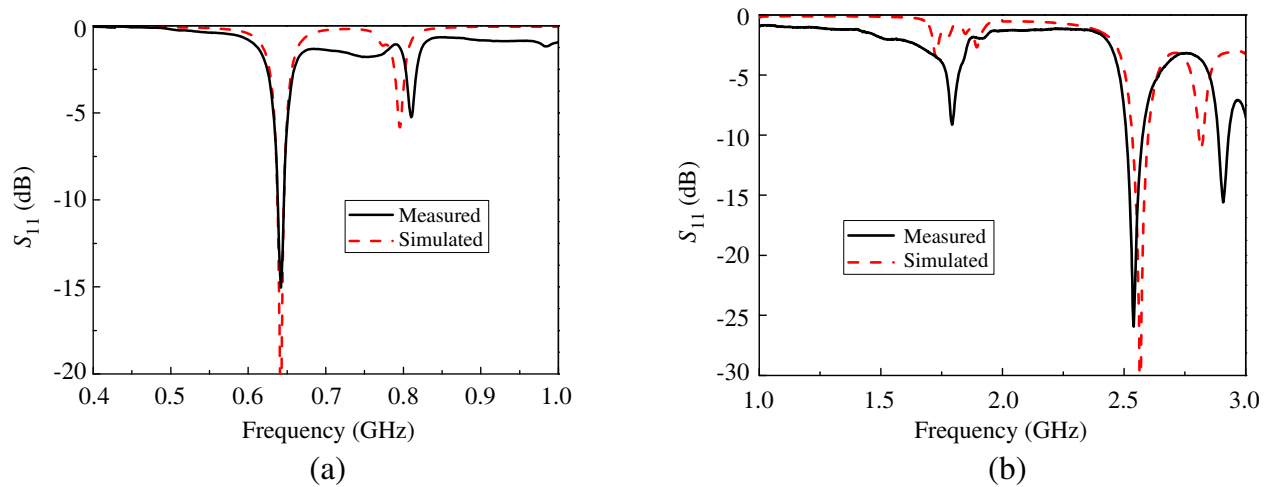


**Figure 9.** Measured and simulated reflection coefficients: (a) in frequency band from 0.4 GHz to 1.0 GHz; (b) in frequency band from 1.0 GHz to 3.0 GHz.

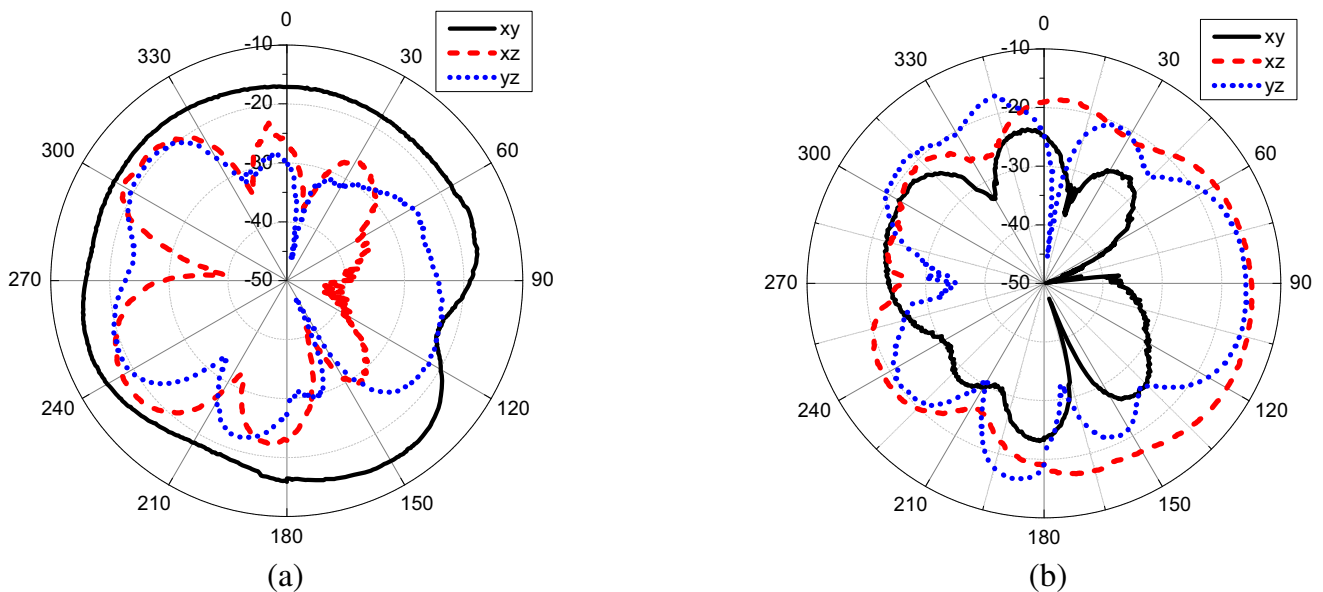


**Figure 10.** Measured radiation patterns at 642 MHz, where the LPA is placed for horizontal polarization in (a) and vertical polarization in (b), respectively.

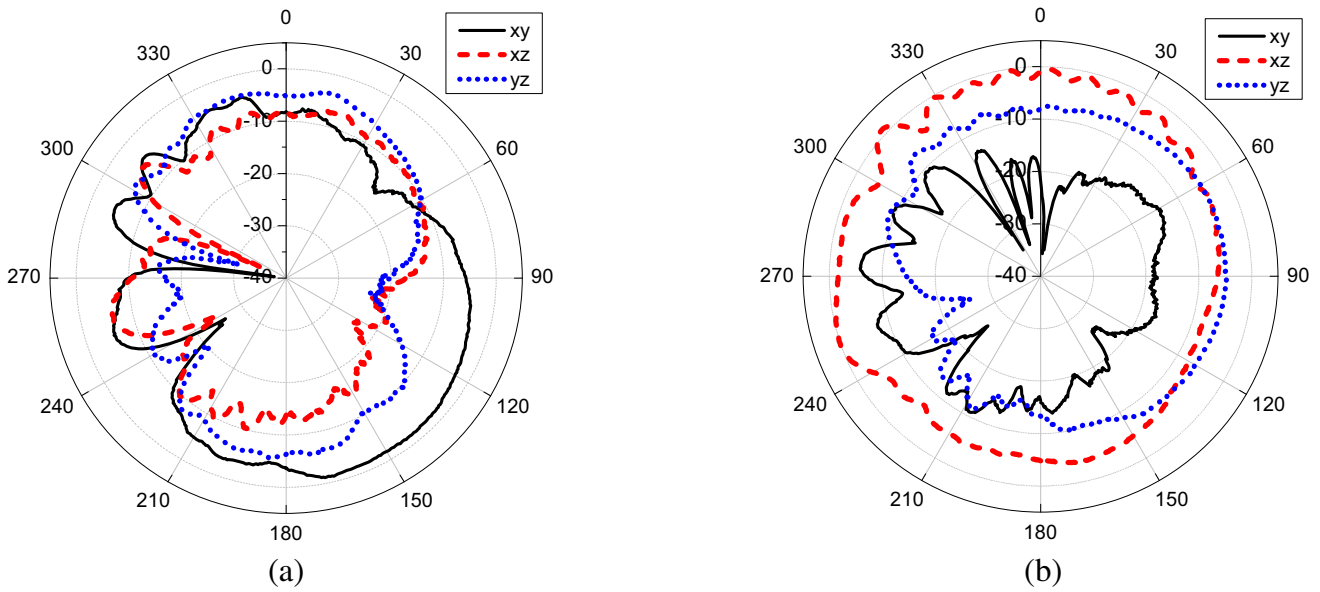


**Figure 11.** Measured radiation patterns at 2.543 GHz, where the LPA is placed for horizontal polarization in (a) and vertical polarization in (b), respectively.

**Table 1.** Summary and comparison of proposed antennas with earlier reported antennas.

	Frequency, GHz	Electrical size	Bandwidth	Gain, dBi	Radiation efficiency*
This work	0.642	$0.055\lambda_0 \times 0.055\lambda_0$	1.17%	-14.3	6.7%*
	2.543	$0.22\lambda_0 \times 0.22\lambda_0$	2.67%	-1	27.2%*
[3]	0.935	$0.081\lambda_0 \times 0.081\lambda_0$	3.61%	-	36.7%
	1.55	$0.134\lambda_0 \times 0.134\lambda_0$	5.55%	-	43.6%
[6]	0.92	$0.15\lambda_0 \times 0.04\lambda_0$	3.3%	-0.92	41.1%
	1.89	$0.31\lambda_0 \times 0.08\lambda_0$	3.7%	-0.67	44.6%
	1.76	$0.117\lambda_0 \times 0.117\lambda_0$	1.4%	2.1	-
[10]	2.55	$0.17\lambda_0 \times 0.17\lambda_0$	1.25%	-3.9	-
	3.85	$0.256\lambda_0 \times 0.256\lambda_0$	2.6%	2.5	-

\* We estimate the radiation efficiency by compare the measured gain and maximum feasible gain calculated by (2).

center frequency equal to 642 MHz. The VSWR < 2.0 bandwidth is about 1.17%, and the second band is located at the center frequency of 2.543 GHz, with corresponding VSWR < 2.0 bandwidth equal to 2.67%. Two standard log-periodic antennas (LPA) covering UHF and S bands are used for radiation pattern measurements. Figure 10 and Figure 11 show the radiation results, and the measured gains are -14.3 dB and -1 dB, respectively. From Equation (2), we can estimate that the maximum feasible gain can reach -2.55 dB at 642 MHz and 4.65 dB at 2.543 GHz. By comparison with the measured gain, the radiation efficiencies are 6.7% and 27.2% at 642 MHz and 2.543 GHz, respectively. Table 1 is prepared to compare the proposed antenna with other reported ESAs in terms of bandwidth, size, and efficiency, from which the design in our work has the smallest size as  $0.055\lambda_0 \times 0.055\lambda_0$  at 642 MHz, and the thickness of antenna is only  $0.0064\lambda_0$ .

## 5. CONCLUSION

In this paper, we design a printed dual-band antenna working in dual-bands. The antenna is fabricated using two layers of substrate. On the top layer, a ring is adopted to excite the antenna. On the other layer, four SRs and one SRR are placed and coupled with the ring, which brings lower resonant frequency and improves the input impedance characteristics. The measurement agrees well with calculation, and the presented antenna is electrically small.

## ACKNOWLEDGMENT

This work was supported in part by the Natural Science Foundation of Hunan Province under Grant 2019JJ50392, the Scientific Research Fund of Hunan Provincial Education Department under Grant 17B160, the China Postdoctoral Science Foundation under Grant 2018M633666, and the National Natural Science Foundation of China for young scholars under Grant 61601478.

## REFERENCES

1. Patel, R. H., A. Desai, and T. Upadhyaya, "A discussion on electrically small antenna property," *Microwave and Optical Technology Letters*, Vol. 57, No. 10, 2386–2388, 2015.
2. Peng, L., P. Chen, A. Wu, and G. Wang, "Efficient radiation by electrically small antennas made of coupled split-ring resonators," *Scientific Reports*, Vol. 6, 33501, 2016.
3. Wang, L., M. Q. Yuan, and Q. H. Liu, "A dual-band printed electrically small antenna covered by two capacitive split-ring resonators," *IEEE Antennas and Wireless Propagation Letters*, Vol. 10, 824–826, 2011.
4. Peng, L., S. Sang, Z. Wang, et al., "Wideband radiation from an offset-fed split ring resonator with multi-order resonances," *IEEE Antennas and Wireless Propagation Letters*, Vol. 17, No. 12, 2198–2202, 2018.
5. Tang, M. C., B. Zhou, Y. Duan, X. Chen, and R. W. Ziolkowski, "Pattern-reconfigurable, flexible, wideband, directive, electrically small near-field resonant parasitic antenna," *IEEE Transactions on Antennas and Propagation*, Vol. 66, No. 5, 2271–2280, 2018.
6. Sharma, S. K., M. A. Abdalla, and Z. Hu, "Miniaturisation of an electrically small metamaterial inspired antenna using additional conducting layer," *IET Microwaves, Antennas & Propagation*, Vol. 12, No. 8, 1444–1449, 2018.
7. Rezaeieh, S. A., M. Antoniadou, and A. M. Abbosh, "Compact wideband loop antenna partially loaded with Mu-negative metamaterial unit cells for directivity enhancement," *IEEE Antennas and Wireless Propagation Letters*, Vol. 14, 1018–1021, 2015.
8. Park, J.-H., Y.-H. Ryu, and J.-H. Lee, "Mu-zero resonance antenna," *IEEE Transactions on Antennas and Propagation*, Vol. 58, No. 6, 1865–1875, 2010.
9. Tang, M. C., Z. Wu, T. Shi, and R. W. Ziolkowski, "Electrically small, low-profile, planar, Huygens dipole antenna with quad-polarization diversity," *IEEE Transactions on Antennas and Propagation*, Vol. 66, No. 12, 6772–6780, 2018.
10. Rahimi, M., F. B. Zarrabi, R. Ahmadian, Z. Mansouri, and A. Keshtkar, "Miniaturization of antenna for wireless application with difference metamaterial structures," *Progress In Electromagnetics Research*, Vol. 145, 19–29, 2014.
11. Harrington, R. F., "Effect of antenna size on gain, bandwidth, and efficiency," *J. Res. National Bureau of Standards, D. Radio Propag.*, Vol. 64D, No. 1, 1–12, 1960.